The Depositional Record
The journal of the International Association of Sedimentologists
Open Access

ORIGINAL RESEARCH ARTICLE

Early diagenetic evolution of Chalk in eastern Denmark

JULIEN MOREAU*, MYRIAM BOUSSAHA*, LARS NIELSEN*, NICOLAS THIBAULT*, CLEMENS V. ULLMANN† and LARS STEMMERIK‡

*Department of Geosciences and Natural Resource Management, University of Copenhagen, Øster Voldgade 10, 1350 Copenhagen, Denmark (E-mail: moreau.juli1@gmail.com)
†Camborne School of Mines, University of Exeter, Penryn Campus, Penryn TR10 9FE, UK
‡Natural History Museum, University of Copenhagen, Øster Voldgade 10, 1350 Copenhagen, Denmark

Keywords
Chalk, deformation bands, Denmark, diagenesis, polygonal faults, stylolites.

Manuscript received: 5 April 2016; Accepted: 13 September 2016

The Depositional Record 2016; 2(2): 154–172

doi: 10.1002/dep2.19

ABSTRACT

The genesis of polygonal faults is an intriguing diagenetic phenomenon. This study discusses their origin in carbonate mudstones together with other associated diagenetic features. In the eastern Danish Basin, at the fringe of the Baltic Sea, the Stevns peninsula offers a unique opportunity to study the early diagenesis of Upper Cretaceous Chalk deposits, buried between 500 m and 1400 m. This paper combines data from onshore and offshore high-resolution seismic reflection profiles, a fully cored borehole with high-resolution wireline logs and quarry and coastal cliff outcrops to study early diagenetic features at different scales. Chalk is affected by an extensive polygonal fault system that is detected in onshore and offshore seismic data. Outcrop and core data provide a better understanding of the distribution of contraction-related features like deformation bands (hairline fractures), stylolites and fluid escape structures. An original model of genetic relationships between these different diagenetic processes is documented for Chalk. The spatial relationships between stylolites and fractures suggest that pressure-solution processes triggered shear failure that initiated the polygonal fault systems. The early diagenetic processes affect the reservoir properties of Chalk by creating compartments and vertical connections. Taking these features into account will allow for a more detailed understanding of early diagenesis and better models for exploiting drinking water or hydrocarbons hosted in Chalk.

INTRODUCTION

Chalk is a singular material consisting principally of an accumulation of micron-sized calcareous nannofossil grains. It is similar to both fine-grained siliciclastic sediments and carbonate bio-accumulations and mechanisms common to both realms can be invoked during early diagenesis (Cartwright *et al.*, 2003; Hibsch *et al.*, 2003; Fabricius & Borre, 2007; Goulty, 2008; Gaviglio *et al.*, 2009; Wennberg *et al.*, 2013). This paper aimed to provide new insights into the first phases of Chalk diagenesis by untangling the complex relationship between centimetre to metre-scale observations made on a fully cored borehole with high-resolution wireline logs, on quarry exposures and on coastal cliff outcrops of the Stevns peninsula (Denmark), and 100 m-scale observations from onshore and offshore high-resolution seismic reflection profiles in the same area.

For this study, the focus is on Chalk from the eastern Danish Basin which reputedly underwent very shallow burial preceding its modern exposure on the Stevns peninsula (Fig. 1; Nielsen *et al.*, 2011). Previous studies of the area have documented the stratigraphy, depositional facies, porosity variations with depth and the associated seismic velocities (Frykman, 2001; Lykke-Andersen & Surlyk, 2004; Stemmerik *et al.*, 2006; Surlyk *et al.*, 2006, 2013; Anderskouv *et al.*, 2007; Esmerode *et al.*, 2007; Nielsen *et al.*, 2011). These studies allow the seismic response of the Chalk to be assessed according to stratigraphic variations and compositional changes, and in particular, the impact on porosity and seismic velocities (Nielsen *et al.*, 2011). Porosity loss, measured directly on core plugs or indirectly with borehole geophysics and seismic refraction data, increases with both burial depth and clay content (Japsen, 2000; Nielsen *et al.*, 2011). According to Wennberg *et al.* (2013), local porosity loss

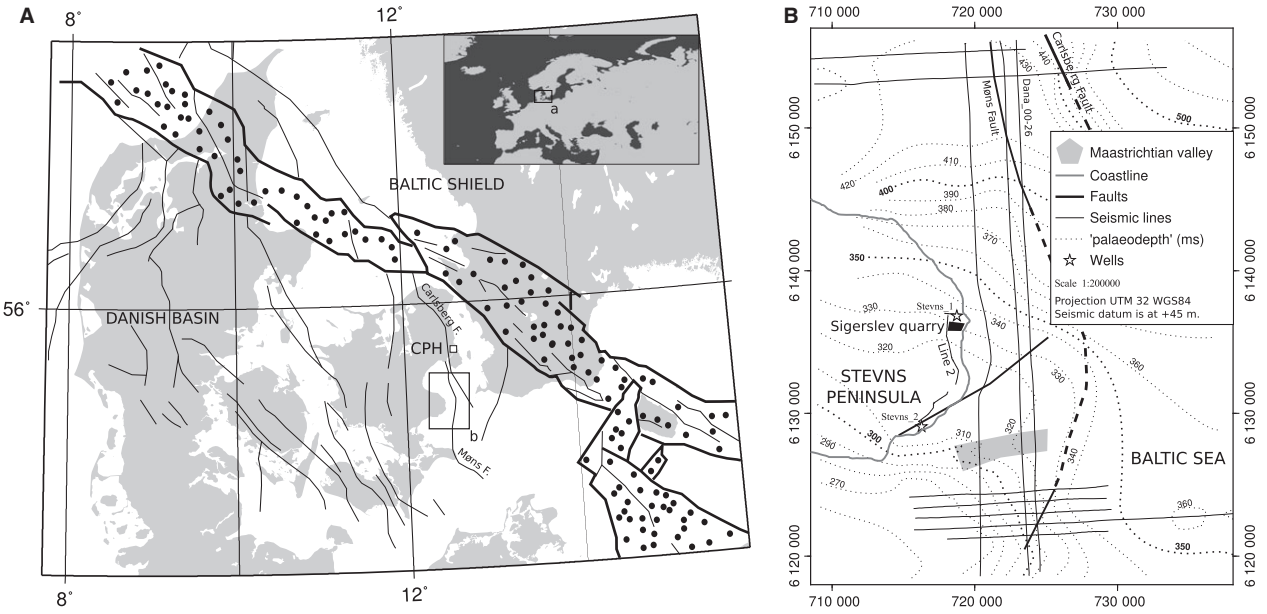

Fig. 1. Location map of the study area. (A) Main faults affecting the top Zechstein, modified from Graversen (2009). The dotted area is the Sorgenfrei-Tornquist zone, the suture where inversion occurs during the Maastrichtian. The Møns Fault is also inverted during that time (this study). CPH = Copenhagen, F. = Fault. Projection UTM 32, coastline from GSHHS database. (B) Location of the seismic lines and wells. Assuming the upper part of the Late Cretaceous in the Stevns peninsula has not been tectonically deformed, one horizon close to the Campanian–Maastrichtian boundary has been picked to represent the palaeo-sea floor depth. The horizon represents the slope of the Late Cretaceous ramp, each dotted line is separated by *ca* 15 m.

also occurs within Chalk deformation bands (hairline fractures). These deformation bands are compaction features corresponding to jointing and local pore-space collapse.

Depending on the methods used, burial depths between 500 m and 750 m have been estimated for the Stevns area based on seismic velocities of Chalk (Japsen & Bidstrup, 1999; Japsen, 2000; Nielsen *et al.*, 2011). The 750 m estimate in Japsen (2000) is based on an extensive data set from Danish offshore and onshore areas showing a direct link between seismic velocity and porosity of Chalk, and assuming a linear porosity reduction during burial. The 500 m estimate in Nielsen *et al.* (2011) is based on the recognition of three discrete steps with increasing velocity at *ca* 100 m, 300 m and 600 m most likely linked to significant diagenetic boundaries and thus implying a stepwise transformation of Chalk.

Polygonal fault systems are regionally extensive normal faults restricted to a specific stratigraphic interval (Cartwright, 2011 and reference therein). The origin of these faults is known to be diagenetic and disconnected from tectonic processes (Henriet *et al.*, 1991), except in one documented case (anticline formation, Petracchini *et al.*, 2015). Several genetic processes have been discussed in the literature and an extensive review can be found in Cartwright (2011). The latest and most accepted model invokes an overall contraction (in opposition to loading-related strain) of the host-rock, where focused grain dissolution weakens high porosity fine-grained sediments and generates shear failure which then propagates into slip and the formation of a fault plane (Shin *et al.*, 2008). The model of Shin *et al.* (2008) was numerically and experimentally conducted and upscaled and compared with 3D seismic data (Shin *et al.*, 2010). Such numerical models have only considered sedimentary rocks dominated by siliciclastic rock dissolution. As documented in this study, however, polygonal fault systems also affect carbonate mudstones and have been documented in multiple basins and settings (Cartwright *et al.*, 2003; Hibsch *et al.*, 2003; Hansen *et al.*, 2004; Cartwright, 2011; Sandrin *et al.*, 2012; Tewksbury *et al.*, 2014).

In this study, seismic reflection profiles were used to describe faults. By combining the seismic interpretation with studies of diagenetic features like hairline fractures, stylolites and flint found in the Stevns-2 core as well as in outcrop, the links between early diagenetic transformations are explored at different scales (Fig. 1). For the first time, it is possible to link polygonal fault systems and deformation bands to the occurrence of stylolites. By including data from a Chalk succession and diagenetic suite, the observations may help to consolidate the realization of a common theory for the formation of polygonal fault systems by grain dissolution during early diagenesis (Shin *et al.*, 2008, 2010; Cartwright, 2011).

GEOLOGICAL SETTING

The Stevns peninsula is located at the transition between the eastern edge of the Danish Basin and the western edge of the Baltic Sea (Fig. 1). Below the Stevns peninsula, a full Mesozoic sedimentary succession is supposedly present (from the Triassic to the Early Paleogene; Erlström *et al.*, 1997). Broadly, the Mesozoic and Cenozoic sedimentary rocks draw a large wedge, opening towards the west in the Central Graben (North Sea) and pinching out in the study area constituting the eastern edge of the subsiding intracratonic area (Lassen & Thybo, 2012). Eastward and southward, the basin progressively deepens again into the Polish Trough and the Sorgenfrei-Tornquist zone (Graversen, 2004; Lassen & Thybo, 2012; Sopher & Juhlin, 2013).

The sedimentary rocks are deformed in narrow zones along WNW-ESE-trending tectonic lineaments, the Rinkøbing-Fyn High in the south and the Tornquist suture in the north (Lassen & Thybo, 2012). Additionally, important NNW-SSE oriented tectonic lineaments, some apparently inverted during the Maastrichtian, have been identified in our data set (Møns Fault; Fig. 1; Graversen, 2009). The latter lineaments have not been previously studied individually. They are parallel to structures characterizing the area such as the Sorgenfrei-Tornquist zone and the Carlsberg Fault, and consequently are believed to have similar, mainly strike-slip, motions (Rosenbom & Jakobsen, 2005; Graversen, 2009). These structures have been active since at least the Palaeozoic and still generate earthquakes (Graversen, 2009; GEUS, 2015; Kammann *et al.*, 2016). Despite the presence of these large tectonic structures in the offshore areas east of the Stevns peninsula, the coastal cliff of the Stevns peninsula is without major fault or internal offsets within strata and the upper Maastrichtian – lower Danian sedimentary rocks are subhorizontal (Surlyk *et al.*, 2006). Analysis of the outcrops highlights the dominance of recent fractures and subhorizontal joints associated with relaxation after ice sheet unloading combined with the local stress field, resulting from the deglaciation of the area (11 to 20 ka; Frykman, 2001; Rosenbom & Jakobsen, 2005). The sediments formerly covering Chalk have been removed after the area was exhumed (Japsen *et al.*, 2007; Nielsen *et al.*, 2011).

This study mainly focuses on the Campanian and Maastrichtian Chalk which has been cored in the Stevns-1 and Stevns-2 boreholes (Figs 1 and 2; Stemmerik *et al.*, 2006). The overall stratigraphy and depositional evolution of the cored succession is presented by Surlyk *et al.* (2013) and a detailed description of the Stevns-2 core is given by Boussaha *et al.* (2016). The Stevns-2 core consists of a lower, *ca* 100 m thick interval of marl-Chalk alternations of Campanian – earliest Maastrichtian age overlain by 70 m of pure white Chalk and 170 m of Chalk with flint bands (Fig. 2C). At the top of the Maastrichtian, bryozoans become more abundant and the flint bands undulate, highlighting the presence of mounds and Chalk waves forming in response to contour currents (Anderskouv *et al.*, 2007). The Maastrichtian is locally terminated by the famous Iridium-rich clay layer characterizing the boundary between the Mesozoic and the Cenozoic although, like in the Stevns-2 core, this may be locally eroded (Surlyk *et al.*, 2006; Boussaha *et al.*, 2016). The last few metres of the Stevns succession are formed by spectacular bryozoan mounds of Danian age (Fig. 2; Bjerager & Surlyk, 2007; Boussaha *et al.*, 2016).

Stylolites have formed through the succession, and carbonate remobilization is observed in some fractures (Fig. 2; Rasmussen & Surlyk, 2012; Surlyk *et al.*, 2013). In the Stevns-1 core, suboptimal preservation of the calcareous nannofossils forming Chalk has been related to partial dissolution caused by fluid migration (Thibault *et al.*, 2012). Such fluid flow within Chalk has also been interpreted as being the cause of brecciation in the Stevns-1 well (Rasmussen & Surlyk, 2012). Although these indicators of chemical and mechanical compaction have been studied (Fabricius & Borre, 2007; Fabricius *et al.*, 2010), relatively little has yet been done to understand their implications for the structural architecture of eastern Denmark Chalk at the regional scale.

Data collection and reporting

This study is based on analyses of seismic reflection profiles, well logs, core and outcrop data (Fig. 1). The seismic sections are high-resolution onshore and offshore data imaging the area of the Stevns peninsula (Fig. 1). The onshore seismic data have a central frequency of 85 Hz. The bin spacing is 2·5 m, and the sampling of the 800 ms (*ca* 1·2 km) long record is done every millisecond. Locally, some acquisition problems disturbed the record (strong winds). In consequence, the stratigraphic patterns are not properly resolved in the east–west sections as well as certain parts of the north–south sections of the onshore survey.

The offshore data have a central frequency of 80 Hz, the bin spacing is 10 m, the traces are 2 s TWT long and sampled every millisecond (Lykke-Andersen & Surlyk, 2004). Ties with the wells Stevns-1 and Stevns-2 are performed using velocities from seismic refraction data, corrected with wireline logs of density and sonic (Nielsen *et al.*, 2011; Figs 1 and 2). The theoretical vertical resolution of the reflection seismic data using the mean velocity of the studied interval is *ca* 8 m (¼ of the wavelength, 2·6 km s^{-1}; Nielsen *et al.*, 2011).

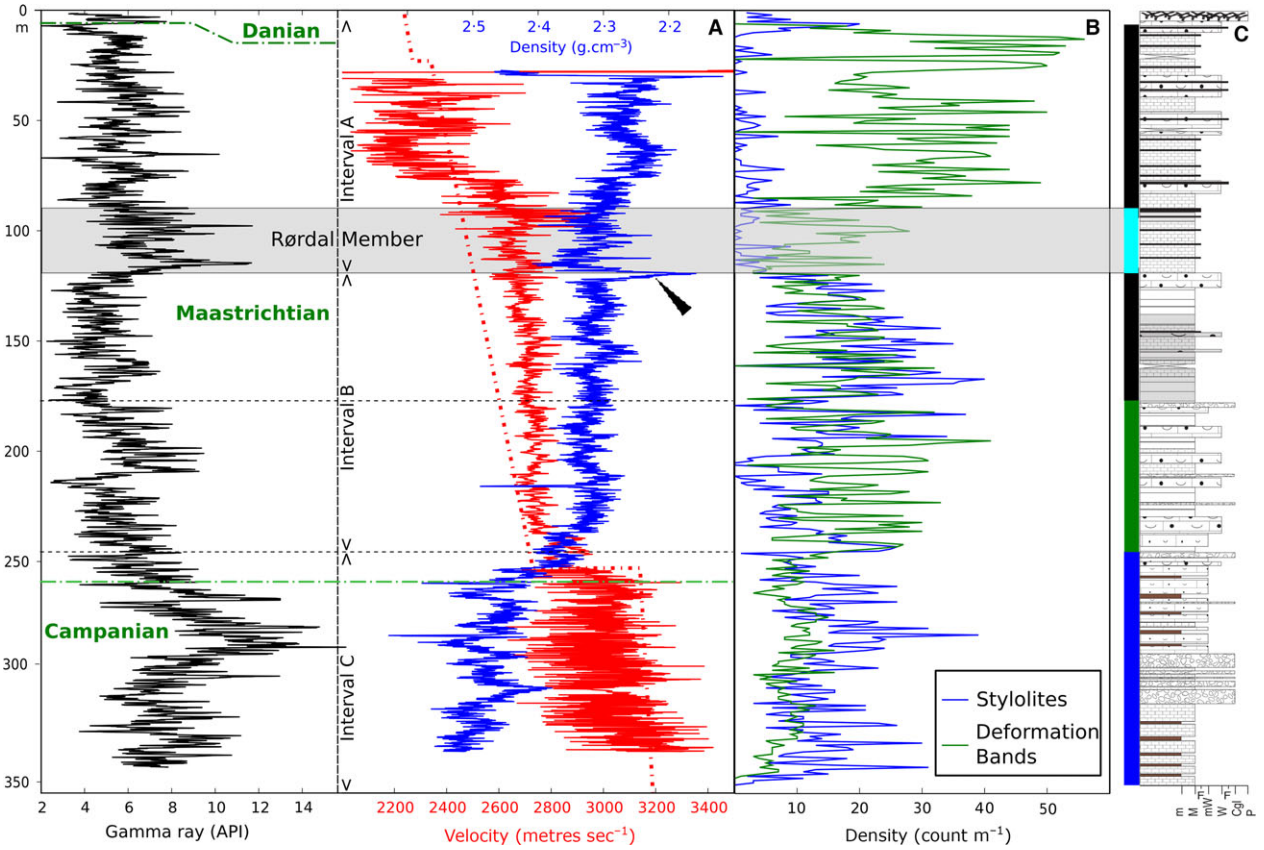

Fig. 2. Petrophysical (A), structural (B) and sedimentological (C) data from the Stevns-2 core. In C, the facies scale is modified from Boussaha *et al.* (2016) with: m = marls, M = mudstones, F = flint, mW = micro-wackestones, W = wackestones, Cgl = Conglomerate, P = packstones. The patterns used in the sedimentary log follow this scale. The sudden rise below a clay-rich interval (grey interval, Rørdal Member) in stylolites is attributed to critical burial depth reached (1 km) and local compartmentalization. Deformation bands (hairlines) may be disappearing with stylolite formation. The drop in density (black arrow) is considered to be the result of the local dissolution of carbonates. Colour codes in C correspond to the colour used in the cross-plots of Fig. 6. [Colour figure can be viewed at wileyonlinelibrary.com]

In the offshore data, a dip-steering median filter has been applied on the lines to favour continuous reflective events along the structural dip but preserving edges (details of the technique in Torvela *et al.*, 2013; www.opendtect.org). After careful picking and filtering, the overall quality of the image is locally good to very good for stratigraphic analysis (Fig. 3). In order to image subtle fracture patterns with small offsets and reflectivity lows in the onshore data, a fault enhancement filter has been used (www.opendtect.org). It is a combination of a (i) dip-steered median filter and a (ii) dip-steered diffusion filter. Broadly, when evaluating data in a dip-steered ellipsoid, if the similarity is high, filter (i) is applied, raising the continuity; whereas if the similarity is low (near a fault), filter (ii) is applied, making a sharp fault break. In order to compare the seismic imaging and the core observations, a linear velocity function is applied to project the well data and convert times measured on the profiles to depth. The function is extracted from the refraction study of Nielsen *et al.* (2011) and corresponds to a starting velocity of 2200 m s^{-1} with an acceleration of 1000 m s^{-2}. The first 50 ms of the onshore seismic profiles contain very intricate reflections which seem to cross-cut and are not present in the lower resolution offshore line. Potential Quaternary incisions/deformations or undetermined artefacts might be the cause of this architecture and the interval is consequently not considered in the final models. Similarly, the presence of sea-bed multiples and multiples of the quaternary sediments overprint the signal offshore and make it difficult to interpret the first 100 ms of the profiles (Fig. 3). A standard seismic stratigraphic technique based on reflection terminations has been applied to visualize seismic sequences in the profiles (Figs 3 and 4). The sequences are constructed based on onlaps onto horizons that truncate the underlying reflections. These horizons highlight the base of seismic sequences within Chalk (alternating colours in Figs 3 and 4). In addition, in order to characterize throw distribution patterns, 125

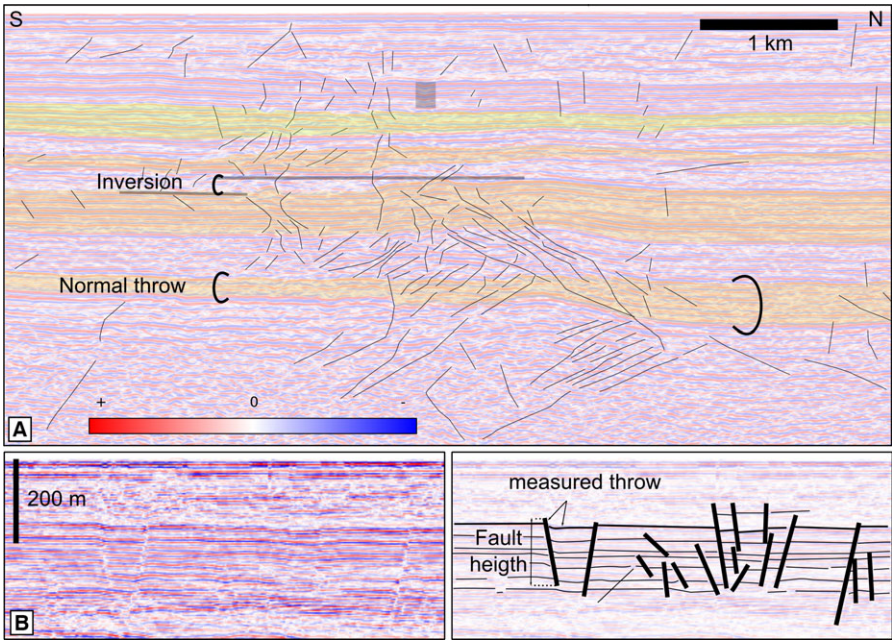

Fig. 3. Details of features and how they were measured from offshore seismic reflection data at a 1 : 1 scale. (A) Example of a section through the Møns Fault (location in Fig. 1) showing its extent across the whole imaged sedimentary succession. Note its complex history with extension at base, followed by inversion and formation of a broad anticline affecting the depositional sequences (marked by the alternating colours). The fault forms a cluster which draws diamond shapes. (B) Example of strata-bound faults (polygonal faults). This figure illustrates the geometric characteristics of the faults (high angle, strata bound), their composite nature and the way the throw and the height are measured. [Colour figure can be viewed at wileyonlinelibrary.com]

fault segments have been measured in the offshore seismic profiles (Fig. 5). These measures are standard for blind-fault analysis with their apparent dips (Fig. 5A), the ratio between the maximum throw and the height (Fig. 5B; Baudon & Cartwright, 2008; Shin *et al.*, 2010; Cartwright, 2011). The throw measured on individual offset reflections as well as the location of maximum observed throw have been plotted against normalized fault plane intersection (with the seismic profile; Fig. 5C). To compensate for the lack of 3D data, Gaussian kernel density estimations are calculated for the values repartition of the ratio between fault height and the maximum throw as well as the throw repartition against the normalized fault plane intersection, giving a statistical vision of the measurements as if they were continuously sampled (colour mapping in Fig. 5). Since the seismic profiles form a suborthogonal grid and because apparent dip angles have a large variability, the seismic grid can be considered as intersected by faults with a large variability of strikes (producing various apparent dip angles). Therefore, the obtained density functions are considered representative of the probability of occurrences in 3D.

The Stevns-1 and -2 boreholes are entirely cored with excellent recovery (>98%; Stemmerik *et al.*, 2006). A suite of geophysical measurements have been logged in the boreholes (spectral gamma ray, neutron density, sonic) and on the core (gamma ray, density). During investigations of the Stevns-2 core particular attention was given to the quantification of structural and diagenetic features and the abundance (i.e. count of occurrence per 1 m interval) of stylolites, marl layers, fractures and joints (deformation bands) has been precisely mapped (Fig. 2). This allows precise correlation of petrophysical data with core-based observations of density of structural and diagenetic features (Figs 2 and 6).

Field work in the Sigerslev Chalk quarry and the nearby coastal sections (Fig. 1) focussed on structural observations and mapping of flint (Supplementary material 1). Since flint bands mostly nucleate very close to the seabed, they mimic the palaeo-sea floor and are the only markers which allow for approximation of the sedimentary architecture in pure Chalk successions (Surlyk *et al.*, 2006; Anderskouv *et al.*, 2007; Madsen & Stemmerik, 2010). In addition, in the otherwise homogeneous Chalk of the study area flint has precipitated in faults and 16 segments exhibiting this have been measured and mapped (Fig. 7). Delineation of the structures in Fig. 8 is made by drawing the flint nodules on a high-resolution panoramic photograph stitched using Hugin software and Panini projections to reduce parallax distortions (http://hugin.sourceforge.net/; Supplementary material 1). However, since the picture is taken from the bottom of the quarry

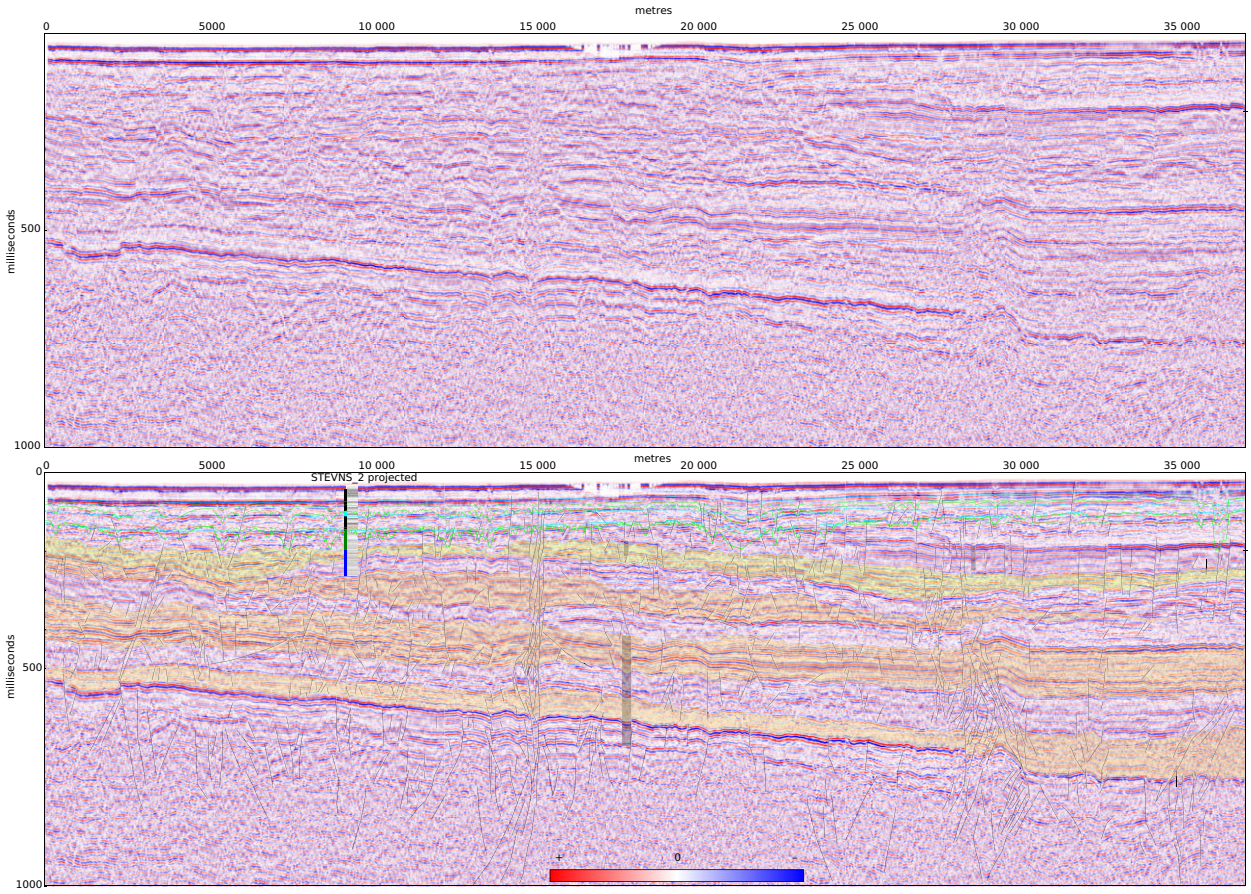

Fig. 4. Seismic interpretation of line Dana 00-26 offshore Stevns peninsula, location in Fig. 1. Blue lines represent the sea-bed multiples with the water–air interface. Green lines are multiples made by the reflection between the quaternary – Chalk and the sea-bed – Chalk interfaces. Thick quaternary sequences are generating push down artefacts locally. The colours are the main seismic sequences observed. The basal sequence probably starts in the Turonian, just above the most pronounced seismic event, marking the base of Chalk deposition in the area (Lykke-Andersen & Surlyk, 2004). The yellow sequence shows Upper Campanian deposition which in the Stevns-2 well corresponds to marl-Chalk alternations. The grey shadings are potential pock mark conduit sections. By comparison with the local stratigraphy some could be traced to the base of the Cretaceous (Erlström *et al.*, 1997). The top of the section has not been interpreted because of the predominance of the multiples over the direct reflections. [Colour figure can be viewed at wileyonlinelibrary.com]

wall, the top of the image remains distorted, and horizontal beds appear convex upward.

Data presentation and interpretation

Seismic observations

The seismic data vary in quality throughout the study area but the stratigraphy can be interpreted and the main reflections can be correlated between offshore and onshore lines (Lykke-Andersen & Surlyk, 2004; Esmerode *et al.*, 2007). However, due to lack of a proper tie, all age attributions older than the upper Campanian should be considered with caution.

Based on the drilled Maastrichtian sedimentary rocks, the seismic reflection pattern on the high-resolution onshore profiles can tentatively be correlated with the broad facies subdivision identified in the nearby Stevns-1 and Stevns-2 cores. There are two end-members in the reflection patterns attributed to (i) high energy (relatively) reflections that are continuous on all seismic profiles and (ii) low reflectivity, chaotic to disrupted reflections (Figs 3, 4 and 9). Onshore, the patterns are correlated with the borehole data and correspond to (i) marl-Chalk alternations and (ii) the 'white Chalk', which is a very pure mud-sized Chalk (Figs 3, 4 and 9). The picked reflections show numerous disruptions in the form of low- to high-angle, transparent and continuous segments from 10 to 100 ms in height (Figs 3, 4 and 9). The segments are completely nonreflective, highlighting fractures that are organized in clusters (e.g. Fig. 9). The

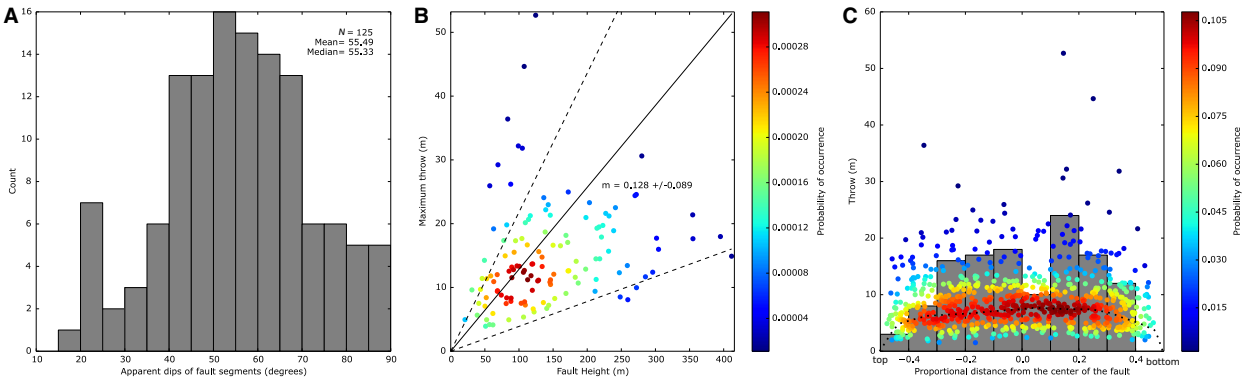

Fig. 5. Geometric characteristics of the 125 measured strata-bound faults. (A) Apparent dip of the fault segments on the seismic profiles. (B) Maximum displacement (throw) versus fault height and the density function of the data point probability of occurrence. The ratio between the two values is very high and indicates probably a high degree of lateral connectivity with other polygonal faults (Shin *et al.*, 2010). (C) The density function in colour shows the distribution of measured throws against the normalized fault height. 0 is at the centre of the faults, 0·5 the lower tip and −0·5 the upper tip. The histogram in the background indicates the position of maximum throws on the normalized fault planes (in count). Both distributions are slightly skewed towards the lower parts, but very mildly. Overall the throws seem equally distributed with a M-type distribution (Baudon & Cartwright, 2008). [Colour figure can be viewed at wileyonlinelibrary.com]

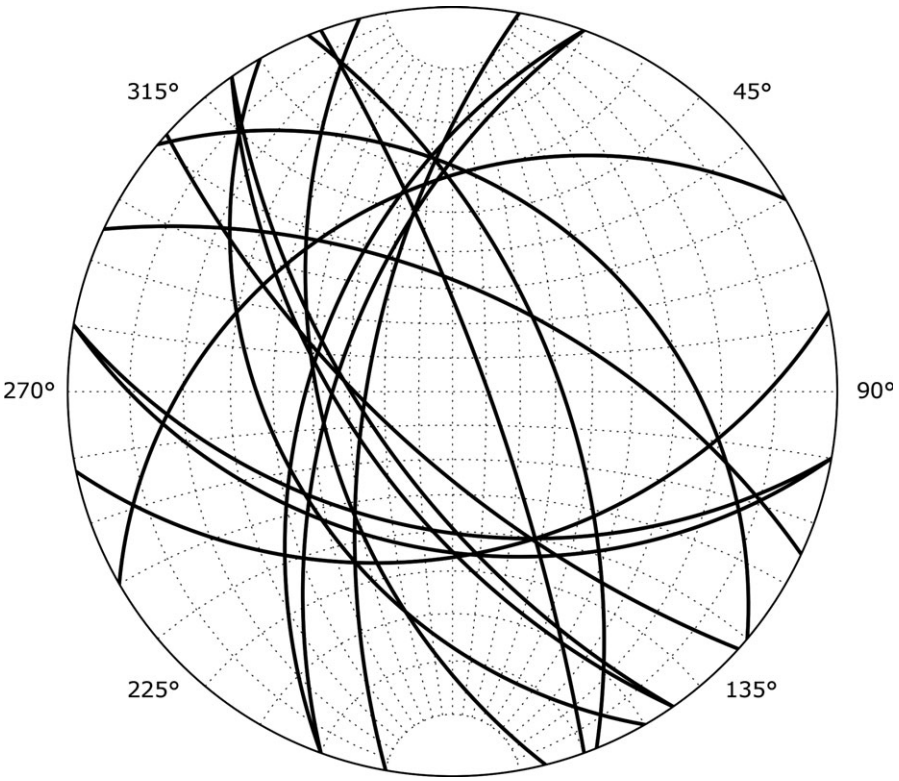

Fig. 6. Cross-plot of Chalk characteristics and features versus sonic velocity in the Stevns-2 well. Colours represent the main Chalk facies from core analysis (cf. Fig. 2). Sonic velocities are from wireline logging. (A) Cross-plot between sonic velocity versus the number of stylolites per metres counted on the core. The plot shows no clear correlation between the amount of (diagenetic) pressure-solution and the sonic velocity. (B) Plot of the sonic velocities against density. The diagram shows a clear trend, however, except when the Chalk contains marls, distinction between the main Chalk facies is not possible based on these two standard wireline tools. (C) Plot of the sonic velocities versus the natural radioactivity wireline log. No clear trend between the clay content and the velocity can be evidenced here.

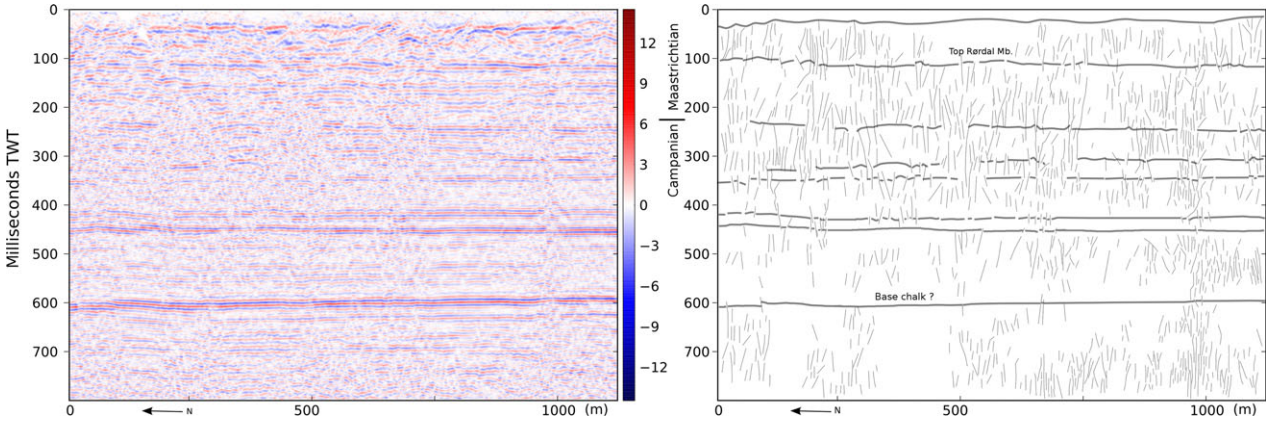

Fig. 7. Stereonet projection of the exposed fault planes marked by flint bands. No preferential orientation is distinguished on these 16 measured planes. [Colour figure can be viewed at wileyonlinelibrary.com]

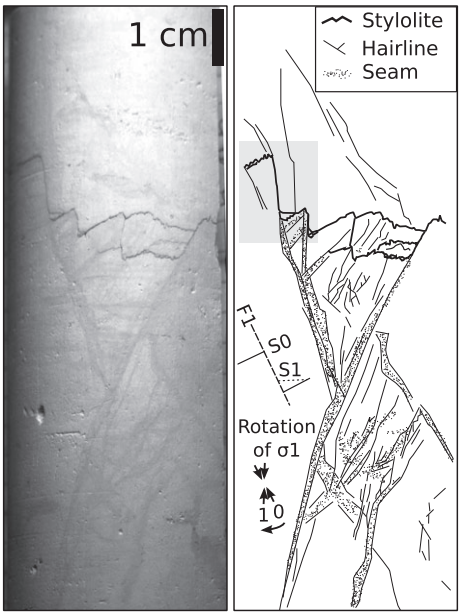

Fig. 8. Relationship between hairlines, stylolites and carbonate seams. The core picture is taken from the Stevns-2 core at 183 m MD. It shows that the stylolites are genetically associated with the hairline fractures. Here, the progressive normal throw is followed by several subtle re-equilibration of the stylolite profile which tries to stay perpendicular to the main stress vectors while the footwall of the fracture rotates (shaded area illustrates the rotation). The carbonate seams start directly under the stylolites and fill the space surrounding the underlying fractures, illustrating the downward carbonate mass transfer associated with the pressure-solution phenomenon. Note that the core is not slabbed, so the surface here is half a cylinder and distortion of the perspective occurs on the side of the picture.

highly reflective events (marl-Chalk alternations) have very few disruptions but larger offsets reaching *ca* 60 m (*ca* 20 ms; Figs 3, 4, 5 and 9). The weakly reflective parts (white Chalk) contain most of the clusters, but contain subtle fault throws (Figs 3, 4 and 9). The faults have an apparent dip distribution which has almost a Gaussian distribution with a mean and a median of *ca* 55° and a standard deviation of 16° (Fig. 5A). The ratio of the fault heights against their observed maximum throw is 0·13 ± 0·09 (Fig. 5B). The throw distribution along the faults is typical M-type (trapezoid-shape) with no clear asymmetry with depth (Fig. 5C; Muraoka & Kamata, 1983; Baudon & Cartwright, 2008). Maximum throws are not necessarily centred on the fault planes and seem more common in the lower part of the faults (histogram, Fig. 5C). The throw distribution is relatively smooth with small throws close to the tip of the faults and relatively constant throws in the main part of the faults (local averages ranging from 5 to 7 m; Fig. 5C). Throws seem to be only slightly larger in the lower half of the faults, making their distribution slightly skewed at the bottom (Fig. 5C). A large part of the clusters have their faults terminating on the relatively strong reflective events without offsetting them (Figs 3B, 4 and 9). On the contrary, some of the clusters have a continuous vertical extension through the whole sedimentary succession and form regional lineaments routed deep below the Chalk Group and imaged in several adjacent profiles (Figs 3A, 4 and 9). The latter clusters have typical diamond-shaped sections (Figs 3A and 4). One cluster shows a complex history during Chalk deposition with a normal throw at the base followed by inversion of the structure and creation of an anticline (fault propagation fold; Figs 3A and 4). Vertically stacked depressions are observed, some of them as deep as the Lower Cretaceous (grey, Figs 3A and 4).

Borehole observations

The wireline log data show an increase in sonic velocity with depth and a corresponding increase in density

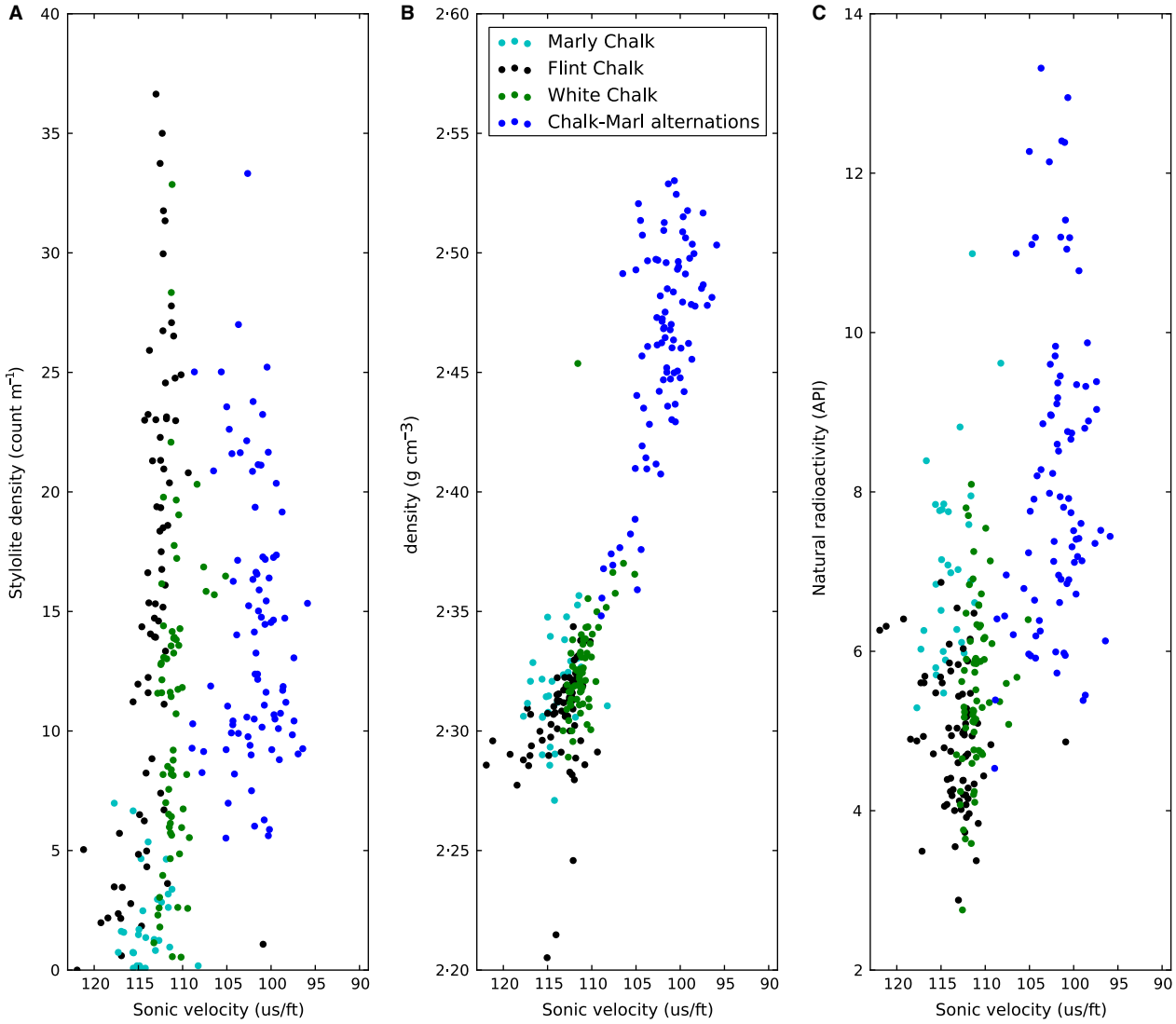

Fig. 9. Seismic interpretation of the line 2 onshore Stevns peninsula, location in Fig. 1. Notice the abundance of small faults between the low reflectivity intervals (e.g. base Maastrichtian) compared to the high reflectivity intervals (e.g. upper Campanian). The high reflectivity layers show drag folds and conical patterns of fault clusters. [Colour figure can be viewed at wileyonlinelibrary.com]

(equals decrease in porosity) confirming the link between seismic velocity and porosity of the Chalk suggested by Japsen (2000; Figs 2B and 3A). However, the increase in sonic velocity is stepwise – as is the increase in density – with major jumps at 75 m MD and 240 m MD (Measured Depth; Fig. 2A). The vertical evolution of the measured velocities indicates a partitioning of the section in three intervals (A, B and C). Interval A is defined by acceleration with depth until 120 m MD (Fig. 2A). Within Interval A, the velocity is very variable with $\pm$200 m s^{-1} high-frequency variations. The base of Interval A is formed by the Rørdal Member, a marly Chalk unit, whereas the top is essentially composed of Chalk with occasional flint bands (Fig. 2). Interval B comprises white Chalk and Chalk with flint layers between 120 m and to 240 m MD (Fig. 2). In this interval, the velocity is stable around 2700 $\pm$ 100 m s^{-1}. Density shows a consequent drop in the first 10 m at the top of Interval B (directly below the Rørdal Mb.; black arrow, Fig. 2A). The interval below 240 m MD forms Interval C and is characterized by higher velocities and densities and by very high-frequency variations (*ca* 3000 $\pm$ 200 m s^{-1} and +0·2 g cm^{-3}; Fig. 2A). Interval C is composed of interbedded marls and Chalk Boussaha *et al.* (2016).

Diagenetic compaction features, consisting mainly of stylolites and deformation bands, have been quantified. Stylolites have classical saw-teeth structures with stylus-shaped teeth reaching maximum amplitudes of a couple

of centimetres. They resemble those described by Lind (1993) from ODP leg 130 where the dark colour is probably due to the accumulation of insoluble material (Fig. 8). The deformation bands, also called 'hairline fractures' in the literature, are also typical of Chalk (Wennberg *et al.*, 2013 and references therein). In the Stevns-2 core, the individual deformation bands are extremely thin and barely visible with the naked eye (consequently probably in the order of 0·1 mm in width; Fig. 8). They can extend over a few millimetres to 10 cm in height (Fig. 8). Some organize in swarms of coalescent parallel fractures making them more visible (Fig. 8), and can also present synthetic/antithetic organizations (Fig. 8). Some of the swarms are surrounded by a diffuse area of darker Chalk attributed to carbonate reprecipitation (carbonate seams, dotted area in Fig. 10). Detailed core observations have been used to understand the geometrical relationships between stylolites, hairlines and carbonate seams (Fig. 8). The hairline fractures (F1; Fig. 8) have a normal throw, offsetting a first generation of stylolites (S0; Fig. 8). A second generation of stylolites (S1) is in today's 'horizontal' position and is developed within the footwall of the fracture plane (Fig. 8). S0 and S1 merge at different angles, S0 being tilted due to the fracture's normal throw. Downward, the pressure-solution structures (stylolites) and the darker Chalk along the hairline fractures indicates the presence of carbonate seams (Fig. 8). There are no seams above the solution structures, they only appear impregnating the fractures downward of the stylolites (Fig. 8).

The quantification of structural and diagenetic features exhibited by the core show that hairline fractures are generally less abundant with depth and have a local minimum at the base of Interval A (Fig. 2B). Interval B (from 120 to 240 m) contains two parts with many fractures that are separated by an interval with very few fractures at 175 m MD (Fig. 2B). This lower fracture density interval corresponds to Chalk with flint/white Chalk transition (black to green; Fig. 2B and C). There is a noticeable drop in the density of deformation bands in Interval C.

The trend of stylolite density with depth contrasts with the distribution of hairline fractures, showing a stepwise overall increase in concentration (Fig. 2B). The stylolite concentration in the uppermost 10 m of the core is higher than in the rest of Interval A (Fig. 2B). The stylolite density increases rapidly at 120 m and shows an overall increase down to 175 m (Fig. 2B). There is a clear distinction between Chalk with flint from 120 to 175 m (more

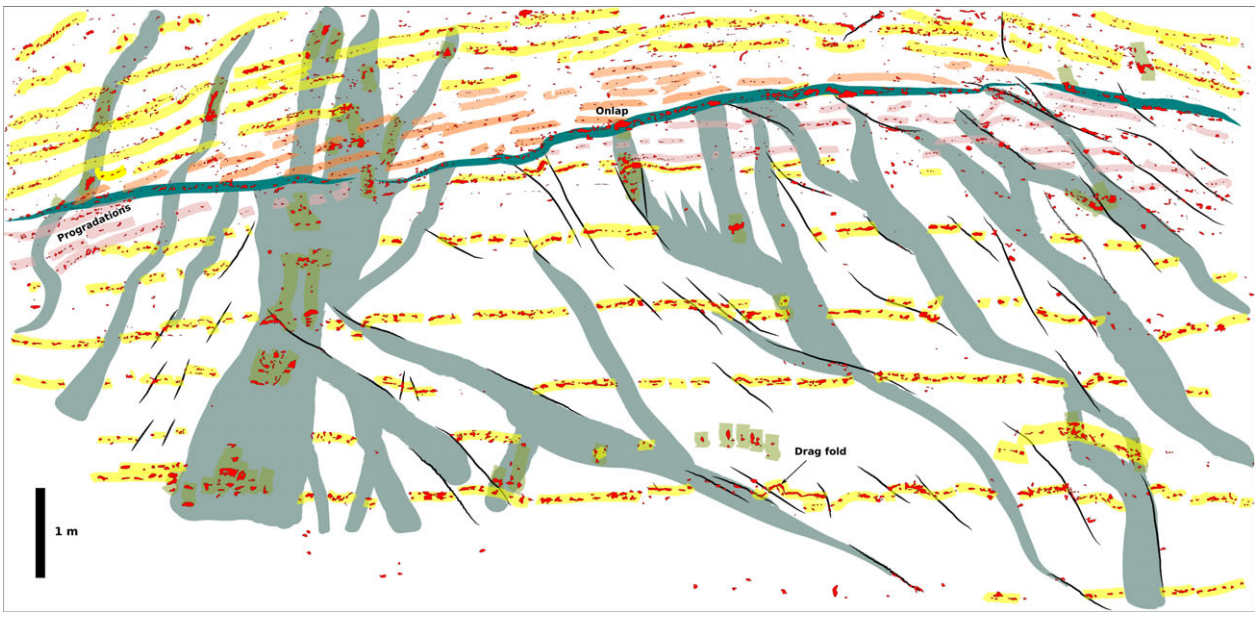

Fig. 10. Interpretation of panoramic pictures taken in the Sigerslev Quarry illustrating the relationship between polygonal faults and fluid expulsion conduits terminating in a pockmark (Fig. 1). All the flint nodules of this quarry face have been drawn in red. Original picture is in the Supplementary material 1. Flint bands showing the regular stratigraphy are in yellow. Areas where paramoudra-like flint structures (green) are present and showing gaps in the (stratigraphic) flint bands are considered as former fluid conduits (blue-grey). Steeply dipping, elongated flint nodules (Fig. 11A and B) and drag folds in flint bed indicate the presence of faults (polygonal, in black). The constructive part of the pockmark spreading out laterally is highlighted by the pink prograding flint bands. The depression of the pockmark is marked by a thick flint band (in turquoise). The filling of the pockmark is highlighted in orange. The filling of the pockmark and the main conduit have a slightly darker colour on the quarry wall (Supplementary material 1). [Colour figure can be viewed at wileyonlinelibrary.com]

stylolites) and pure white Chalk from 175 to 240 m (less stylolites, Fig. 2B and C). The bottom of the core (>240 m MD) has a variable density of stylolites with around 15 per metre.

Cross-plotting sonic velocities and density shows a good correlation and a clear separation between marls and purer Chalk (Fig. 6B). The cross-plot between stylolite density and sonic velocity in Fig. 6A shows that there is no correlation between these two parameters. This lack of relationship is also well illustrated in the interval from 120 to 240 m in Fig. 2 where the almost stable density and sonic velocity of Chalk (Fig. 2A) contrasts with the pronounced variations in stylolite density (Fig. 2B). The relationship between the sonic velocity and the natural radioactivity, which should represent the clay content, is also poorly developed (Fig. 9C). Overall, except when Chalk contains a high concentration of marl (deep blue Fig. 6), Chalk facies do not show any trend or correlation with the number of stylolites (i.e. intensity of diagenesis) or clay content (detrital input; Fig. 6).

Field observations

Chalk exposed in Sigerslev Quarry and the adjacent coastal cliffs shows spectacular palaeo-sea-bed topographies mimicked by undulating flint bands within Chalk (Anderskouv *et al.*, 2007). Locally, the flint bands are cross-cut at a high angle by flint aligned within planes which locally offset the strata (Figs 10 and 11). The stratigraphic flint bands are locally absent along these planes which occasionally exhibit small drag folds in their immediate vicinity (Fig. 10). The subvertical zones lacking stratiform flint bands (blue-grey in Fig. 10) contain cylindrical hollow flints resembling *Batichnus paramoudrae* (green in Fig. 10; Bromley *et al.*, 1975). Most of the subvertical zones end at a level marked by a particularly thick flint band (turquoise in Fig. 10). This thick band is topped by an interval containing low-angle dipping flint bands (pink in Fig. 10). The pink interval depicted in Fig. 10 seems to be constructive and grows laterally away from the biggest subvertical zone (small progradations; Fig. 8). The thick flint band delineates the base of a specific infill which is slightly greyish in colour (in orange and onlapping on the thick turquoise flint band in Fig. 8; supplementary material 1). The flint bands cross-cut the stratigraphy at high angles highlighting planes that are rarely continuously visible over more than 2 m (Fig. 11A). The planes themselves are composite and show different orientations of segments (Fig. 11B). They are difficult to measure and access, so no statistical measurement could be done but it seems that the structures have no clear preferred orientation (Fig. 7).

At the bottom of the quarry another important structure intersects the stratigraphy: a 10 cm thick cluster of stylolites can be followed continuously on the quarry walls (Fig. 11C and D). This first (in burial depth) continuous stylolite is located just below the structures observed in Fig. 10. Other stylolites which are discontinuous and not subparallel to the stratigraphy are observed at the top of the quarry (Fig. 11E).

Careful observations and cleaning of the quarry wall highlight numerous fractures and deformation structures (Fig. 11F, G, and H). Subhorizontal decollement planes have been observed, separating intervals with differential horizontal motion (Fig. 11F). Hairline fractures are observed all over the exposures as long as Chalk has enough colour contrast and markers to show the offsets (Fig. 11G and H). Fractures organized in conical sets are observed with kinematic indicators showing important volume changes (Fig. 11G). Small faults in the prolongation of the flint bands signify normal throws but also folding in the vicinity of the fault (Fig. 11H). Both of these features underline the importance of contractional volume changes (Fig. 11H).

DISCUSSION

The seismic data show the presence of two types of faults. Regionally extensive fault clusters affecting the whole imaged succession, being subparallel to the Sorgenfrei-Tornquist and the Carlsberg fault zones, are considered to be similar strike-slip lineaments (e.g. at 15 000 and 30 000 m in Fig. 4). The presence of an anticline and the differential sedimentation associated with it indicate an originally normal throw followed by inversion during Campanian times (Fig. 4). It is assumed that the regional fault system is not associated with the diagenesis of Chalk and follows the general history of the North Sea Basin (Erlström *et al.*, 1997; Japsen *et al.*, 2007; Sopher & Juhlin, 2013), and its analysis is considered out of the scope of this study.

Insights from strata-bound fault geometries on seismic data

Strata-bound faults (Figs 4 and 9), characteristic of polygonal fault systems (Cartwright *et al.*, 2003), are the second type encountered. The throw distribution analysis shows that fault geometry is very similar to other polygonal fault systems or more broadly to blind faults (Baudon & Cartwright, 2008). The dips of most measured faults range from 40° to 70° (Fig. 5A). This dip range is slightly less steep than faults forming close to the sea-bed (50° to 80°) but still much steeper than the faults forming at depth (20 to 50°; Cartwright, 2011). Knowing that Chalk

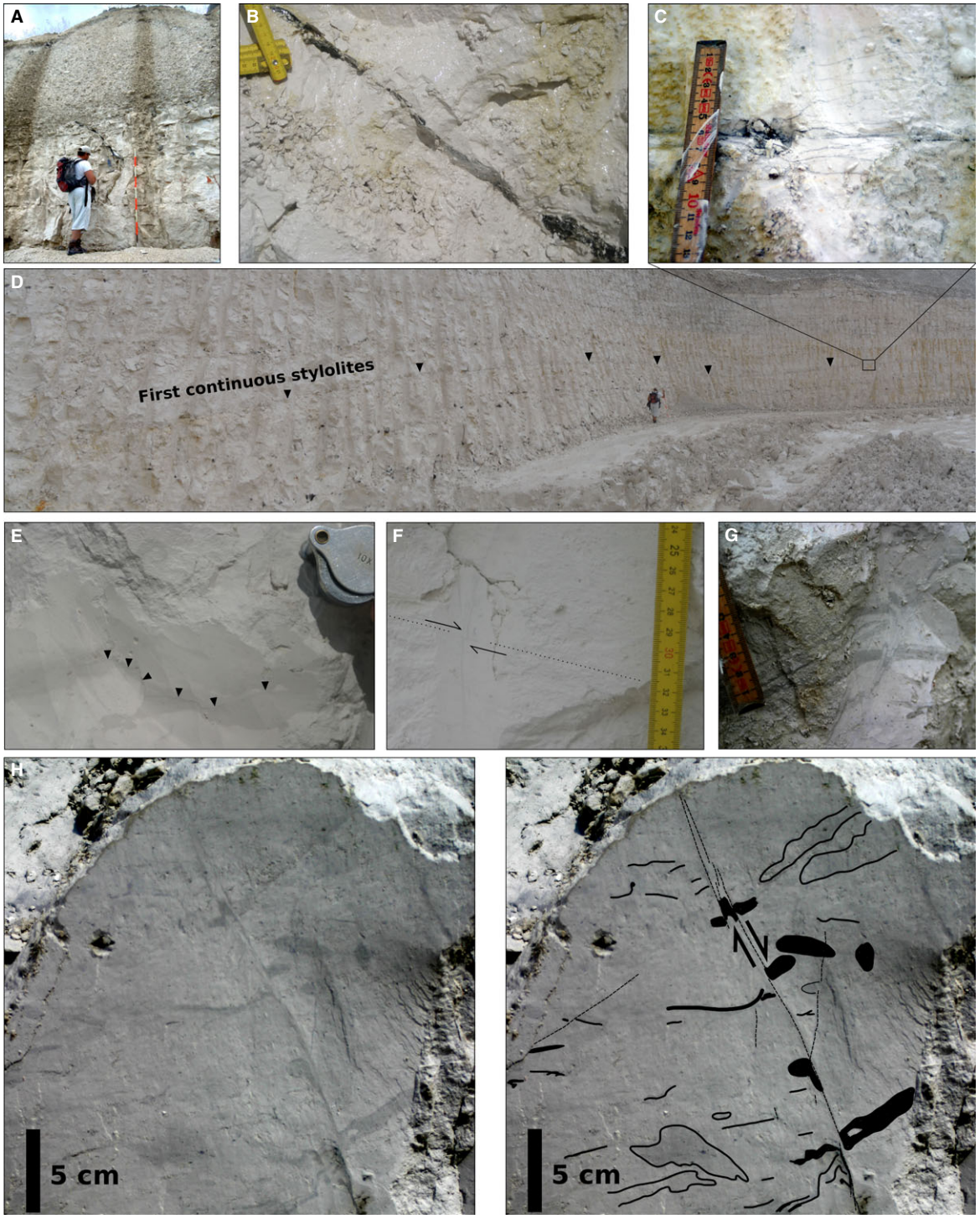

Fig. 11. Small-scale diagenetic features at the Sigerslev Quarry and surroundings. (A) 2 m long flint band within a polygonal fault at the coastal cliff. (B) Flint precipitation within a polygonal fault. Notice the discontinuity of the nodules and the absence of internal fractures. Scale in cm. (C) Close up view of the cluster of continuous stylolites situated at the very bottom of the quarry. Scale in cm. (D) Panoramic view of the first continuous stylolites. Note that they are not parallel with the flint bands (original stratigraphy). (E) Small-scale stylolite from the upper part of the quarry. (F) Decollement plane between two intervals with small subhorizontal offset in the deepest part of the quarry. (G) Hairline fractures organized in conical shape illustrating the contraction of the sediment. Scale in cm. (H) Normal fault within Chalk. The footwall is contracted at the contact with the fault. [Colour figure can be viewed at wileyonlinelibrary.com]

succession has probably reached burial depths of *ca* 500 m in the study area (Nielsen *et al.*, 2011), it can be assumed that compactional flattening with burial has made the dips shallower than their original formation geometry (Cartwright, 2011; Nielsen *et al.*, 2011). Therefore, it is possible to conclude that the faults were originally steeper, formed close to the sea-bed and were consecutively flattened by compaction. Since the maximum displacement of polygonal faults crudely scales with the fault height, this ratio is established to compare with other systems by plotting the maximum throw versus the height of individual faults (Fig. 5B; Shin *et al.*, 2010; Cartwright, 2011). The measured faults have a very large ratio of fault height to maximum throw of 0·128 ± 0·089 which is significantly higher than the standard ratio for polygonal faults of 0·045 ± 0·016 (Shin *et al.*, 2010). Since listric geometries associated with a weak basal layer are lacking, the faults probably have a high degree of lateral intersection (Shin *et al.*, 2010). The throw distribution along normalized distance on the fault planes is an indicator of fault displacement (Fig. 5C; Baudon & Cartwright, 2008; Cartwright, 2011). The displacement gradient starts abruptly from the tip of the faults, is broadly smooth in the central part and slightly more accentuated in the lower half of the faults, and in this sense similar to other studied polygonal fault systems (Fig. 5C; Cartwright, 2011). The M-type displacement pattern characterizes blind-faults and is found in polygonal fault systems (Baudon & Cartwright, 2008; Shin *et al.*, 2010; Cartwright, 2011). The maximum displacement occurs more frequently at the base of the faults; however, it seems to be highly variable (Fig. 5C). This is interpreted as being driven by heterogeneity of the mechanical properties in the sediment pile and a complex growth history (Baudon & Cartwright, 2008). The finite heterogeneous vertical displacement is most probably the result of several 'simultaneous' fault nucleations at different stratigraphic levels that link together vertically and also laterally since the faults have a high degree of intersection (large throw to height ratio). Lateral hard links between polygonal faults will limit their propagations and might be responsible for some large differences between the observed lateral displacement in Fig. 5C (Lonergan *et al.*, 1998). Therefore, it can be suggested that the largest displacements are close to the nucleation points of the faults, where the shear failure occurred. Polygonal faults are interpreted as being associated with contraction of the sediments during burial. Their initiation can be very early in the diagenetic sequence since some are considered active today at the sea-bed (Cartwright *et al.*, 2003; Goulty, 2008). The strata-bound faults are best developed in intervals, which – from correlation to the Stevns boreholes – are known to consist of relatively pure Chalk. In contrast, faulting is rare in intervals composed of Chalk containing marl layers (Fig. 4). The contrasting intensity of faulting in these two rock types indicates different diagenetic response during burial as discussed further below. This intense faulting in the white Chalk facies may be the reason for its poor reflectivity, the seismic waves being scattered by subvertical fault planes.

Relationships between faults, fractures, stylolites and fluid flows

Strata-bound faults are also observed in outcrop (Figs 10 and 11). Measurement of the faults in the field did not reveal a preferred orientation (Fig. 7). Observations of the Chalk of the eastern Danish Basin at all scales, from core and field observations to seismic profiles, highlight the link between the different diagenetic features and illustrate the transformation of the Chalk during its early burial history. Four main controls on the diagenesis can be observed: faults, fractures, stylolites and fluid escape structures.

The faults contain flint which indicates that they were associated with migration of the silica-loaded fluids and therefore formed at relatively shallow depths before opal-CT was transformed to α-quartz (Hibsch *et al.*, 2003; Madsen & Stemmerik, 2010).

The hairline fractures observed in cores and outcrop are similar to the deformation bands described by Wennberg *et al.* (2013). Deformation bands are joints in the Chalk which correspond to local pore-space collapse and are associated with the progressive burial of the sediment (Wennberg *et al.*, 2013). Surprisingly, they reduce in frequency with depth and drop considerably in abundance as stylolites become prominent (Fig. 2). This could indicate that there is a genetic link between hairline fractures and stylolites and that the joints are precursors to the stylolites. When the joints form, the pore space collapses between Chalk grains. Such collapses increase the contact area between the associated grains, facilitating the later pressure-solution processes associated with stylolite formation. While progressing through Chalk, the stylolites assimilate and dissolve the joints so that the higher the number of stylolites observed, the less precursory joints have been preserved (Fig. 2). The link between fractures and stylolites is illustrated in Fig. 8 where there is a discrepancy between the orientation of the fractures (joints) above and below the stylolite. Since it is improbable that stylolites accommodated horizontal displacement, the joints can be considered to be originally organized in a coherent synthetic-antithetic compactional configuration. Only the activity of the stylolite has modified the volumes, dissolving Chalk downward to obtain the observed structural discrepancy above and below the stylolite

(Fig. 8). In addition, the presence of subhorizontal S1 and tilted S0 stylolites along a fracture indicates that the fracture developed in conjunction with S0 (Fig. 8). S0 was originally horizontal and formed perpendicular to the main stress, the lithostatic pressure (vertical). Since the footwall of the fractures became tilted (including S0), the stylolites were not in equilibrium with the main stress, causing a new generation of horizontal stylolites (S1) to form. The rotation of the palaeo-stress indicator (stylolite) is seen as the result of the time-transgressive formation of stylolites in contracting sediment.

The compaction of the solid parts of Chalk and the increasing stylolitization during burial do not result in cementation of the sediment, indicating that the carbonate enriched solutions and the pore water were able to move. In a closed system, the density should rise because pore-space progressively disappears and the dissolved carbonate will re-precipitate as cement. Open-system carbonate mass-transfers match the observations better. This is supported by the absence of correlation between stylolite abundance and density of Chalk in the interval from 120 to 240 m (Figs 2 and 6). It is assumed that the pore water and the carbonate-rich fluids expressed during the formation of stylolites, built up pressure in the sediment which was then released by venting at a given threshold. This was not a continuous process and was most probably focussed over specific stratigraphic intervals. The difference in fault activity between pure Chalk intervals and intervals of interbedded Chalk and marl, together with the pronounced stepwise velocity jumps across these facies transitions, indicate that primary facies had a major influence on diagenesis and resulting variations in fluid pressures during early burial. However, the localization of these intervals is not completely resolved in our data set. Discrete zones characterized by variable preservation of the calcareous nannofossil assemblages have been observed in the Stevns-1 core (Thibault *et al.*, 2012), and may be candidates for localized fluid flow zones.

The significance of cold seeps

In outcrop, evidence of venting is seen as subvertical conduits and strata-bound faults capped by a thick layer of flint (Fig. 10). The flint most likely was precipitated close to the sea floor at a stable redox boundary (Madsen & Stemmerik, 2010), and judging from the flint band orientations above and below, it formed at a time of shifting depositional conditions (Fig. 10; Supplementary material 1). Based on the architectural data, it is proposed that the plumbing system is likely to have been via cold seep. Cold seeps or so-called pockmarks are structures commonly observed in seismic images in association with polygonal fault systems (Fig. 10; Cartwright *et al.*, 2003; Gay *et al.*, 2006) or exceptionally preserved in desert exposures (Tewksbury *et al.*, 2014). The conduits may be the results of fluid expulsions which locally promote the formation of flint in the form of paramoudra-like structures (the vertically stacked hollow flint cylinders; Fig. 10). Polygonal faults generally help drain fluids from depth to the sea-bed (Gay *et al.*, 2006; Tewksbury *et al.*, 2014). Most of the conduits stop within depressions or polygonal faults (Fig. 8). This indicates that the polygonal faults have reached the sea-bed and may have promoted the drainage of fluids through the low permeability Chalk. Similar-sized vertically superimposed depressions are observed on the seismic profiles and are interpreted as being fluid escape structures associated with cold seeps (Figs 3 and 4). The formation of such pockmarks may be quite common in Chalk although not easily observed in the field. Some examples of strata-bound/polygonal faults as well as pockmarks have been documented in seismic data of the North Sea and other basins with thick Chalk accumulations (Gemmer *et al.*, 2002; Hansen *et al.*, 2004; van Gent *et al.*, 2010; Sandrin *et al.*, 2012) and once in the field (Tewksbury *et al.*, 2014). In addition, igneous intrusions and ash layers are documented within the Upper Cretaceous of the nearby Scania area as well as in the Kattegat (Norling & Bergström, 1987; Ziegler, 1987). While cooling down, a volcanic intrusion at depth could also be a potential source of fluids which would have flowed upward through the upper Cretaceous sediments and stimulated the formation of vents, diagenetic reactions and polygonal fault networks (Planke *et al.*, 2005; Gay *et al.*, 2012).

From contraction to shear failure

The data presented here indicate that the hairline fractures are associated with volume change and contraction of Chalk. Observation of millimetre-scale horizontal movements additionally suggests separation in intervals even at small scale (Fig. 11F, G, and H). These characteristics are shared with polygonal fault systems (Cartwright *et al.*, 2003). It is therefore tempting to see deformation bands and polygonal faults as the results of the same processes of contraction of Chalk, just reflecting different scales and locations. These deformation bands reflect a more pervasive deformation than the polygonal faults.

Recently, it has been suggested that diagenetic dissolution of grains is the driving process for polygonal fault system nucleation (Shin *et al.*, 2010; Cartwright, 2011). The sediments involved have low post-peak shear strength (Shin *et al.*, 2010). To achieve this process, the sediments should have a high porosity and be very fine-grained while undergoing mineral dissolution (Shin *et al.*, 2010), conditions which are met in the studied Chalk; the grain

size being less than 20 μm, porosities between 35% and 50% (Frykman, 2001; Nielsen *et al.*, 2011) and the presence of stylolites (pressure-solution structures) attesting to mineral dissolution. In addition, numerical experiments based on this dissolution/shear failure model predict displacement patterns which are strikingly similar to our measured displacement (Fig. 5C; Shin *et al.*, 2010). Therefore, this process is considered the main trigger of contraction-driven faults in the area.

Synthesis

Chalk, like other low permeability, high porosity and very fine-grained sediments, undergoes intense diagenetic transformations in the first stage of its burial history (Fig. 12; Cartwright *et al.*, 2003; Hibsch *et al.*, 2003). A scenario for these transformations can be established from coupled observations of core material, outcrops and seismic profiles in eastern Denmark. Pure white Chalk appears massive but is pervasively disturbed by deformation bands during shallow burial (Fig. 12). At depth, the deformation bands will progressively merge to become stylolites. The stylolites promote mass-transfers of the carbonates, trigger shear failure and the formation of polygonal fault systems (Fig. 12). The polygonal faults propagate to eventually reach the sea-bed, allowing for drainage of overpressured pore water from Chalk and eventually forming pockmarks (Fig. 12). All these processes contribute to the shrinkage of Chalk and can trigger positive feedback cycles. The initiation, temporal progression and termination of this phenomenon, however, are at present not understood.

As also emphasized by Hibsch *et al.* (2003), some faults contain flint nodules, indicating that fluid migration occurred before transformation of opal-CT to α-quartz (Madsen & Stemmerik, 2010). The formation of flint nodules is thought to be a relatively shallow and early

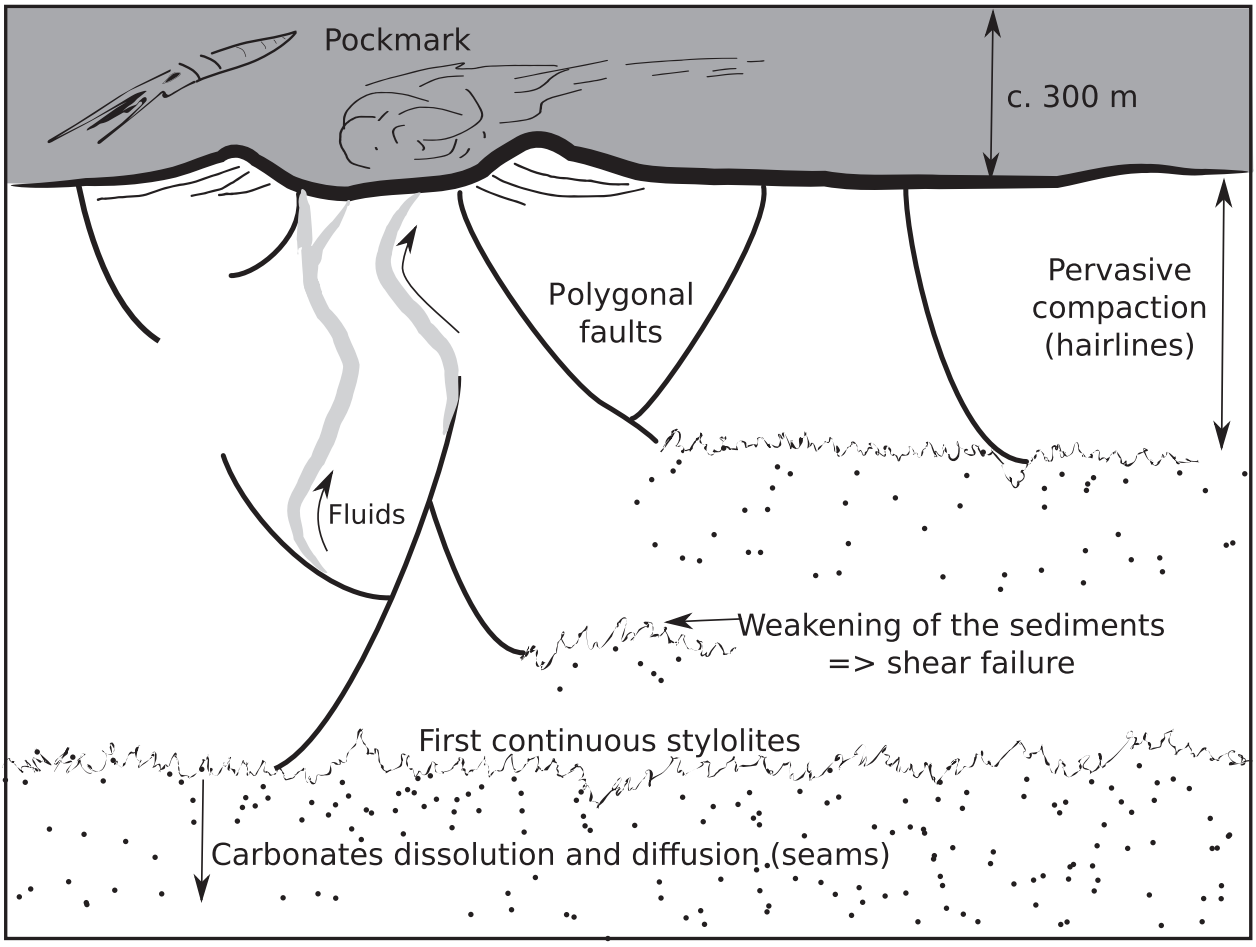

Fig. 12. Model of the positive feedback mechanisms associated with the early diagenesis of Chalk in the eastern Danish Basin. The zone of precipitation of silicates forming the flint bands is not represented here since it has not been quantified and it is probably out of scale (few tens of metres).

diagenetic process although no quantitative estimation has yet been provided for the Stevns peninsula setting (Madsen & Stemmerik, 2010).

In modern Chalk, the formation of 'large' stylolites starts at *ca* 830 m of burial, whereas the first 'small' stylolites occur at 490 m (Lind, 1993). In Sigerslev Quarry, the first large continuous stylolite occurs near the base of the quarry, corresponding to a burial depth of *ca* 580 m, while in Stevns-2 a sudden increase in stylolite concentration occurs at 120 m MD corresponding to a burial depth of 620 m using data in Nielsen *et al.* (2011). It is therefore tempting to assume that a burial depth of *ca* 600 m was needed to trigger the formation of faults and their propagation in the Upper Cretaceous Chalk. This is somewhat shallower than the depth at which modern large stylolites start to form. However, the presence of compartments of different permeability, the heterogeneity of Chalk itself as well as potential fluid supply from deeper parts of the succession may change the initial conditions of stylolite formation in the study area compared to the present-day systems (Lind, 1993). If the estimate of 600 m overburden is applied, nucleation of polygonal faults may have started in the deepest parts of the Chalk Group already during the late Campanian, whereas a late Maastrichtian age is obtained if 800 m of overburden is used as a critical value. In both cases the outlined venting system was in place during the latest stages of Chalk deposition at Stevns (Fig. 12).

The integration of observations from different sources and at different scales have helped to better understand the timing and linking of the processes involved in the transformation of oceanic ooze into Chalk. Better quantitative estimates of the palaeo-burial depths and conditions needed to achieve the observed diagenetic processes could possibly be acquired using a high-resolution 3D seismic data set from an area where Chalk has not been buried more than 1 to 2 km. Another approach would be to use numerical modelling to simulate the dynamics of polygonal faulting in conditions similar to those of the Late Cretaceous of the eastern Danish Basin in order to better constrain the diagenetic sequence affecting Chalk. The velocity layering of Chalk (Fig. 2; Nielsen *et al.*, 2011) indicates that the diagenetic transformations took place at critical depths. This compares to studies of modern ooze from the Java Plateau where the first stylolites occur at 490 m, large stylolites appear at 830 m and cementation starts around 1100 m (Fabricius & Borre, 2007). Evidently, only the deepest parts of the Chalk Group at Stevns have experienced overburdens of more than 1100 m. Considering seismic velocities, Nielsen *et al.* (2011) similarly suggested that an equivalent to the Java Plateau 1100 m event could correspond to a velocity jump identified *ca* 250 m below TD of Stevns-2 (at 600 m today's depth). The rapid increase in velocity at *ca* 240 m and the associated decrease in porosity may be a candidate for such a transformation of intensified dissolution and eventual nucleation of polygonal faults. Most probably, the upper part of Chalk at Stevns had only been affected by one generation of the contraction process associated with the faults, whereas the deeper intervals may have been subject to several generations of faults and consequently, more intense compaction. Is the velocity layering the result of multiple generations of polygonal fault systems or does it represent a stepwise diagenetic evolution of Chalk? This question could be elucidated with a thorough study of deeper buried Chalk successions.

CONCLUSIONS

This study illustrates the diagenetic processes affecting nannofossil ooze in the first kilometre of burial. The diagenetic reactions involve a first stage of pervasive contraction marked by the formation of deformation bands also commonly called hairline fractures. This stage is followed by the start of stylolite formation at *ca* 600 m of burial. For the first time, it can be shown that Chalk behaves like its fine-grained siliciclastic counterparts, and that grain dissolution triggers the formation of polygonal faults. The polygonal faults in the study area have a high degree of lateral connection and form close to the surface. In addition to mimicking the sea-bed, flint bands are fossilized vertical conduits of fluid escape and fault planes, in connection with the polygonal fault system. Like in other polygonal fault systems, the contraction of Chalk was probably associated with cold seeps. Our detailed observations of the diagenetic structures in Chalk of the Stevns Peninsula may have been overlooked elsewhere and should be visible on other good Chalk exposures.

Chalk is a major reservoir for hydrocarbons and drinking water in the North Sea and its coastal areas. Its reservoir properties are influenced by the diagenetic features which are observed in the Stevns peninsula (pore-space collapse, compartmentalization, vertical conduits). However, more quantitative data are needed to better constrain the diagenetic system. Therefore, illustrating the complex interaction of diagenetic phenomena affecting Chalk during burial is expected to stimulate more research on this outstanding sedimentary system.

ACKNOWLEDGEMENTS

We acknowledge Kresten Anderskouv for his pre-review work. Finn Surlyk is thanked for the stimulating discussions on Chalk depositional system and its evolution in Denmark. We would like to thank Lars Ole Boldreel for giving access to the original seismic data repository. Lise

Boulicault is also thanked for her help during field acquisition. We are grateful to Maersk Oil for having sponsored this research in the C-cubed project framework. We thank J. Cartwright, C. Jackson, L. Lonergan and A. Gay for their revision of a former version of the manuscript. We also would like to thank J. D'Arcy for the English-language proofing of the manuscript.

CONFLICT OF INTEREST

No conflict of interest declared.

References

Anderskouv, K., Damholt, T. and **Surlyk, F.** (2007) Late Maastrichtian chalk mounds, Stevns Klint, Denmark – combined physical and biogenic structures. *Sed. Geol.*, **200**, 57–72. doi:10.1016/j.sedgeo.2007.03.005.

Baudon, C. and **Cartwright, J.A.** (2008) 3D seismic characterisation of an array of blind normal faults in the Levant Basin, Eastern Mediterranean. *J. Struct. Geol.*, **30**, 746–760. doi:10.1016/j.jgs.2007.12.008.

Bjerager, M. and **Surlyk, F.** (2007) Danian Cool-Water Bryozoan Mounds at Stevns Klint, Denmark – a new class of non-cemented skeletal mounds. *J. Sed. Res.*, **77**, 634–660. doi:10.2110/jsr.2007.064.

Boussaha, M., Thibault, N. and **Stemmerik, L.** (2016) Integrated stratigraphy of the late Campanian – Maastrichtian in the Danish Basin: revision of the Boreal calcareous nannofossil zonation. *Newsl. Stratigr.*, **49**, 337–360. doi:10.1127/nos/2016/0075.

Bromley, R.G., Schulz, M.-G. and **Peake, N.B.** (1975) *Paramoudras: Giant Flints, Long Burrows and the Early Diagenesis of Chalks*. Kommissionær Munksgaard, København, 42 pp.

Cartwright, J. (2011) Diagenetically induced shear failure of fine-grained sediments and the development of polygonal fault systems. *Mar. Pet. Geol.*, **28**, 1593–1610. doi:10.1016/j.marpetgeo.2011.06.004.

Cartwright, J., James, D. and **Bolton, A.** (2003) The genesis of polygonal fault systems: a review. *Geol. Soc. London. Spec. Publ.*, **216**, 223–243. doi:10.1144/GSL.SP.2003.216.01.15.

Erlström, M., Thomas, S.A., Deeks, N. and **Sivhed, U.** (1997) Structure and tectonic evolution of the Tornquist Zone and adjacent sedimentary basins in Scania and the southern Baltic Sea area. *Tectonophysics*, **271**, 191–215.

Esmerode, E.V., Lykke-Andersen, H. and **Surlyk, F.** (2007) Ridge and valley systems in the Upper Cretaceous chalk of the Danish Basin: contourites in an epeiric sea. *Geol. Soc. London. Spec. Publ.*, **276**, 265–282. doi:10.1144/GSL.SP.2007.276.01.13.

Fabricius, I.L. and **Borre, M.K.** (2007) Stylolites, porosity, depositional texture, and silicates in chalk facies sediments. Ontong Java Plateau, Gorm and Tyra fields, North Sea. *Sedimentology*, **54**, 183–205. doi:10.1111/j.1365-3091.2006.00828.x.

Fabricius, I.L., Bächle, G.T. and **Eberli, G.P.** (2010) Elastic moduli of dry and water-saturated carbonates – effect of depositional texture, porosity, and permeability. *Geophysics*, **75**, 65–78. doi:10.1190/1.3374690.

Frykman, P. (2001) Spatial variability in petrophysical properties in Upper Maastrichtian chalk outcrops at Stevns Klint, Denmark. *Mar. Petrol. Geol.*, **18**, 1041–1062. doi:10.1016/S0264-8172(01)00043-5.

Gaviglio, P., Bekri, S., Vandycke, S., Adler, P.M., Schroeder, C., Bergerat, F., Darquennes, A. and **Coulon, M.** (2009) Faulting and deformation in chalk. *J. Struct. Geol.*, **31**, 194–207. doi:10.1016/j.jsg.2008.11.011.

Gay, A., Lopez, M., Cochonat, P., Séranne, M., Levaché, D. and **Sermondadaz, G.** (2006) Isolated seafloor pockmarks linked to BSRs, fluid chimneys, polygonal faults and stacked Oligocene-Miocene turbiditic palaeochannels in the Lower Congo Basin. *Mar. Geol.*, **226**, 25–40. doi:10.1016/j.margeo.2005.09.018.

Gay, A., Mourgues, R., Berndt, C., Bureau, D., Planke, S., Laurent, D., Gautier, S., Lauer, C. and **Loggia, D.** (2012) Anatomy of a fluid pipe in the Norway Basin: initiation, propagation and 3D shape. *Mar. Geol.*, **332–334**, 75–88. doi:10.1016/j.margeo.2012.08.010.

Gemmer, L., Huuse, M., Clausen, O.R. and **Nielsen, S.B.** (2002) Mid-Palaeocene palaeogeography of the eastern North Sea basin: integrating geological evidence and 3D geodynamic modelling. *Basin Res.*, **14**, 329–346. doi:10.1046/j.1365-2117.2002.00182.x.

van Gent, H., Back, S., Urai, J.L. and **Kukla, P.** (2010) Small-scale faulting in the Upper Cretaceous of the Groningen block (The Netherlands): 3D seismic interpretation, fault plane analysis and regional paleostress. *J. Struct. Geol.*, **32**, 537–553. doi:10.1016/j.jsg.2010.03.003.

GEUS (2015) Tabel med fakta om registrerede danske jordskælv. Registrerede jordskælv. Available at: http://www.geus.dk/DK/nature-climate/natural-disasters/seismology/Sider/seismo_reg-dk.aspx.

Goulty, N.R. (2008) Geomechanics of polygonal fault systems: a review. *Petrol. Geosci.*, **14**, 389–397. doi:10.1144/1354-079308-781.

Graversen, O. (2004) Upper Triassic-Lower Cretaceous seismic sequence stratigraphy and basin tectonics at Bornholm, Denmark, Tornquist Zone, NW Europe. *Mar. Pet. Geol.*, **21**, 579–612. doi:10.1016/j.marpetgeo.2003.12.001.

Graversen, O. (2009) Structural analysis of superposed fault systems of the Bornholm horst block, Tornquist Zone, Denmark. *Bull. Geol. Soc. Den.*, **57**, 25–49.

Hansen, D.M., Shimeld, J.W., Williamson, M.A. and **Lykke-Andersen, H.** (2004) Development of a major polygonal fault system in Upper Cretaceous chalk and Cenozoic mudrocks of the Sable Subbasin, Canadian Atlantic margin. *Mar. Pet. Geol.*, **21**, 1205–1219. doi:10.1016/j.marpetgeo.2004.07.004.

Henriet, J.P., De Batist, M.D. and **Verschuren, M.** (1991) Early fracturing of Paleogene clays, southernmost North Sea: relevance to mechanisms of primary hydrocarbon migration. In: *Generation, Accumulation and Production of Europe's Hydrocarbons* (Ed. A.M. Spenser), *Spec. Publ. Eur. Assoc. Petrol. Geol.*, **1**, 217–227.

Hibsch, C., Cartwright, J., Hansen, D.M., Gaviglio, P., Andre, G., Cushing, M., Bracq, P., Juignet, P., Benoit, P. and **Allouc, J.** (2003) Normal faulting in chalk: tectonic stresses vs. compaction-related polygonal faulting. *Geol. Soc. London. Spec. Publ.*, **216**, 291–308. doi:10.1144/GSL.SP.2003.216.01.19.

Japsen, P. (2000) Investigation of multi-phase erosion using reconstructed shale trends based on sonic data. Sole Pit axis, North Sea. *Global Planet. Change*, **24**, 189–210. doi:10.1016/S0921-8181(00)00008-4.

Japsen, P. and **Bidstrup, T.** (1999) Quantification of late Cenozoic erosion in Denmark based on sonic data and basin modelling. *Bull. Geol. Soc. Den.*, **46**, 79–99.

Japsen, P., Green, P.F., Nielsen, L.H., Rasmussen, E.S. and **Bidstrup, T.** (2007) Mesozoic-Cenozoic exhumation events in the eastern North Sea Basin: a multi-disciplinary study based on palaeothermal, palaeoburial, stratigraphic and seismic data. *Basin Res.*, **19**, 451–490. doi:10.1111/j.1365-2117.2007.00329.x.

Kammann, J., Hübscher, C., Boldreel, L.O. and **Nielsen, L.** (2016) High-resolution shear-wave seismics across the Carlsberg Fault zone south of Copenhagen – implications for linking Mesozoic and late Pleistocene structures. *Tectonophysics*, **682**, 56–64. doi:10.1016/j.tecto.2016.05.043.

Lassen, A. and **Thybo, H.** (2012) Neoproterozoic and Palaeozoic evolution of SW Scandinavia based on integrated seismic interpretation. *Precambr. Res.*, **204–205**, 75–104. doi:10.1016/j.precamres.2012.01.008.

Lind, I.L. (1993) Stylolites in chalk from Leg 130, Ontong Java Plateau. In: *Proceedings of the Ocean Drilling Program, Scientific Results* (Eds W. H. Berger, L. W. Kroenke, T. R. Janecek, and W. V. Sliter), pp. 445–451. Ocean Drilling Program, College Station, TX.

Lonergan, L., Cartwright, J. and **Jolly, R.** (1998) The geometry of polygonal fault systems in Tertiary mudrocks of the North Sea. *J. Struct. Geol.*, **20**, 529–548.

Lykke-Andersen, H. and **Surlyk, F.** (2004) The Cretaceous-Palaeogene boundary at Stevns Klint, Denmark: inversion tectonics or sea-floor topography? *J. Geol. Soc. London*, **161**, 343–352. doi:10.1144/0016-764903-021.

Madsen, H.B. and **Stemmerik, L.** (2010) Diagenesis of Flint and Porcellanite in the Maastrichtian Chalk at Stevns Klint, Denmark. *J. Sed. Res.*, **80**, 578–588. doi:10.2110/jsr.2010.052.

Muraoka, F. and **Kamata, H.** (1983) Displacement distribution along minor fault traces. *J. Struct. Geol.*, **5**, 483–495.

Nielsen, L., Boldreel, L.O., Hansen, T.M., Lykke-Andersen, H., Stemmerik, L., Surlyk, F. and **Thybo, H.** (2011) Integrated seismic analysis of the Chalk Group in eastern Denmark – implications for estimates of maximum palaeo-burial in southwest Scandinavia. *Tectonophysics*, **511**, 14–26. doi:10.1016/j.tecto.2011.08.010.

Norling, E. and **Bergström, J.** (1987) Mesozoic and Cenozoic tectonic evolution of Scania, southern Sweden. In: *Compressional Intra-Plate Deformations in the Alpine Foreland* (Ed. P.A. Ziegler), *Tectonophysics*, **137**, 7–19.

Petracchini, L., Antonellini, M., Billi, A. and **Scrocca, D.** (2015) Syn-thrusting polygonal normal faults exposed in the hinge of the Cingoli anticline, northern Apennine, Italy. *Front. Earth Sci.*, **3**, 1–24.

Planke, S., Rasmussen, T., Rey, S.S. and **Myklebust, R.** (2005) Seismic characteristics and distribution of volcanic intrusions and hydrothermal vent complexes in the Vøring and Møre basins. In: *Petroleum Geology: North-West Europe and Global Perspectives Proceedings of the 6th Petroleum Geology Conference* (Eds A.G. Doré and B.A. Vining), *Geol. Soc. London*, 833–844.

Rasmussen, S.L. and **Surlyk, F.** (2012) Facies and ichnology of an Upper Cretaceous chalk contourite drift complex, eastern Denmark, and the validity of contourite facies models. *J. Geol. Soc.*, **169**, 435–447. doi:10.1144/0016-76492011-136.

Rosenbom, A.E. and **Jakobsen, P.R.** (2005) Infrared thermography and fracture analysis of preferential flow in Chalk. *Vadose Zone J.*, **4**, 271–280. doi:10.2136/vzj2004.0074.

Sandrin, A., Fehmers, G., Printz, B., van Buchem, F., Uldall, A. and **Hoffmann, U.** (2012) Polygonal Faulting in Chalk – an example at the Tyra Field, Danish North Sea. EAGE, Extended Abstracts, 74th EAGE Conference & Exhibition incorporating SPE EUROPEC 2012, Copenhagen, Denmark, 4–7 June 2012.

Shin, H., Santamarina, J.C. and **Cartwright, J.A.** (2008) Contraction-driven shear failure in compacting uncemented sediments. *Geology*, **36**, 931–935. doi:10.1130/G24951A4.

Shin, H., Santamarina, J.C. and **Cartwright, J.A.** (2010) Displacement field in contraction-driven faults. *J. Geophys. Res.*, **115**, 2156–2202. doi:10.1029/2009JB006572.

Sopher, D. and **Juhlin, C.** (2013) Processing and interpretation of vintage 2D marine seismic data from the outer Hanö Bay area, Baltic Sea. *J. Appl. Geophys.*, **95**, 1–15. doi:10.1016/j.jappgeo.2013.04.011.

Stemmerik, L., Surlyk, F., Klitten, K., Rasmussen, S.L. and **Schovsbo, N.H.** (2006) Shallow core drilling of the Upper Cretaceous Chalk at Stevns Klint, Denmark. *Geol. Surv. Denmark Greenland Bull.*, **10**, 13–16.

Surlyk, F., Damholt, T. and **Bjerager, M.** (2006) Stevns Klint, Denmark: Uppermost Maastrichtian chalk, Cretaceous-Tertiary boundary, and lower Danian bryozoan mound complex. *Bull. Geol. Soc. Den.*, **54**, 1–48.

Surlyk, F., Rasmussen, S.L., Boussaha, M., Schiøler, P., Schovsbo, N.H., Sheldon, E., Stemmerik, L. and **Thibault, N.** (2013) Upper Campanian-Maastrichtian holostratigraphy of the eastern Danish Basin. *Cretac. Res.*, **46**, 232–256. doi:10.1016/j.cretres.2013.08.006.

Tewksbury, B.J., Hogan, J.P., Kattenhorn, S.A., Mehrtens, C.J. and **Tarabees, E.A.** (2014) Polygonal faults in chalk: insights from extensive exposures of the Khoman Formation, Western Desert, Egypt. *Geology*, **42**, 479–482.

Thibault, N., Harlou, R., Schovsbo, N., Schiøler, P., Minoletti, F., Galbrun, B., Lauridsen, B.W., Sheldon, E., Stemmerik, L. and **Surlyk, F.** (2012) Upper Campanian-Maastrichtian nannofossil biostratigraphy and high-resolution carbon-isotope stratigraphy of the Danish Basin: towards a standard $\delta^{13}C$ curve for the Boreal Realm. *Cretac. Res.*, **33**, 72–90. doi:10.1016/j.cretres.2011.09.001.

Torvela, T., Moreau, J., Butler, R.W.H., Korja, A. and **Heikkinen, P.** (2013) The mode of deformation in the orogenic mid-crust revealed by seismic attribute analysis. *Geochem. Geophys. Geosyst.*, **14**, 1069–1086. doi:10.1002/ggge.20050.

Wennberg, O.P., Casini, G., Jahanpanah, A., Lapponi, F., Ineson, J., Wall, B.G. and **Gillespie, P.** (2013) Deformation bands in chalk, examples from the Shetland Group of the Oseberg Field, North Sea, Norway. *J. Struct. Geol.*, **56**, 103–117. doi:10.1016/j.jsg.2013.09.005.

Ziegler, P.A. (1987) Late Cretaceous and Cenozoic intra-plate Deformations in the Alpine foreland – a geodynamic model. In: *Compressional Intra-Plate Deformations in the Alpine Foreland* (Ed. P.A. Ziegler), *Tectonophysics*, **137**, 389–420.

Supporting Information

Additional Supporting Information may be found online in the supporting information tab for this article:

Figure S1. Panoramic picture used to draw the flint nodules of Fig. 9.

